Endocr (2010) 37:303–311
DOI 10.1007/s12020-009-9294-8

ORIGINAL ARTICLE

Rosiglitazone improves pancreatic mitochondrial function in an animal model of dysglycemia: role of the insulin-like growth factor axis

Jennifer E. Bruin · James J. Petrik · Jillian R. Hyslop · Sandeep Raha · Mark A. Tarnopolsky · Hertzel C. Gerstein · Alison C. Holloway

Received: 19 October 2009 / Accepted: 21 December 2009 / Published online: 8 January 2010

Abstract Thiazolidinediones (TZDs) improve insulin sensitivity and maintain beta cell mass. This study examined whether this effect is attributable to improved mitochondrial function in the pancreas and the potential involvement of the pancreatic insulin-like growth factor (IGF) axis in mediating this effect. Female Wistar rats were given either saline (vehicle) or nicotine (1 mg kg^{-1} day^{-1}) during pregnancy and lactation. Following weaning, nicotine-exposed offspring were randomized to receive either vehicle or rosiglitazone (3 mg kg^{-1} day^{-1}) until 26 weeks of age when serum and pancreas tissue were collected. The effect of rosiglitazone on nicotine-induced mitochondrial dysfunction was also examined in vitro. Fetal and neonatal nicotine exposure resulted in structural and functional mitochondrial deficits relative to saline controls. The nicotine-induced mitochondrial defects were attenuated by postnatal rosiglitazone administration. A similar effect was observed in vitro; nicotine (25 ng/ml) inhibited beta cell mitochondrial function and co-treatment with rosiglitazone (1 μM) restored enzyme activity to control levels. Fetal and neonatal nicotine exposure also altered key components of the adult pancreatic IGF axis, an effect that was not prevented by rosiglitazone treatment. Rosiglitazone treatment maintains mitochondrial structure and function in the pancreas of rats that are prone to diabetes, as well as mitochondrial function in beta cell culture. We propose that this may be an important part of the mechanism by which rosiglitazone improves beta cell mass and prevents diabetes in individuals with impaired glucose tolerance and/or impaired fasting glucose. The underlying mechanism through which rosiglitazone targets the mitochondria remains to be determined, but does not appear to involve the IGF axis.

Keywords Mitochondria · Rosiglitazone · Pancreas · Type 2 diabetes · Insulin-like growth factors · Nicotine

J. E. Bruin · J. R. Hyslop · A. C. Holloway (✉)
Reproductive Biology Division, Department of Obstetrics and Gynecology, McMaster University, Hamilton, ON L8N 3Z5, Canada
e-mail: hollow@mcmaster.ca

J. J. Petrik
Department of Biomedical Sciences, University of Guelph, Guelph, ON N1G 2W1, Canada

S. Raha · M. A. Tarnopolsky
Department of Pediatrics, McMaster University, Hamilton, ON L8N 3Z5, Canada

M. A. Tarnopolsky · H. C. Gerstein
Department of Medicine, McMaster University, Hamilton, ON L8N 3Z5, Canada

Introduction

Individuals diagnosed with type 2 diabetes are unable to produce enough insulin to maintain normal glucose homeostasis [1]. This insulin insufficiency has been attributed, in part, to reduced beta cell mass and impaired beta cell function [1, 2], both of which are regulated by mitochondria. In the pancreas mitochondrial-mediated apoptosis is a major pathway through which beta cell mass may be regulated [3, 4]. In addition, mitochondria are crucial for maintaining beta cell function through the coupling of a glucose stimulus to insulin release [5–7]. Indeed, isolated islets from transgenic mice with beta cell-specific mitochondrial defects, exhibit reduced glucose-stimulated insulin secretion (GSIS) [8]. Furthermore,

islets from humans and rodents with type 2 diabetes have impaired mitochondrial function [9–11].

Maintenance of beta cell mass and function also depends on the pancreatic insulin-like growth factor (IGF) system, which includes the ligands, IGF1 and IGF2, and receptors, IGF1R, IGF2R and the insulin receptor (IR). Mice lacking either IR or IGF1R in beta cells develop glucose intolerance associated with defective GSIS [12, 13]. Furthermore, when both IR and IGF1R are absent in beta cells, mice are born with normal beta cell mass, but display increased postnatal beta cell apoptosis and a gradual age-dependent decline in beta cell mass [14]. Furthermore, IGF1 and IGF2 have been shown to protect beta cell mass and function, as well as glucose homeostasis in animal and human studies [15–17]. In humans, circulating IGF1 levels are significantly lower in patients with metabolic syndrome [18], and treatment with recombinant IGF1 has been shown to lower glucose levels in both healthy and diabetic individuals (reviewed in [19]).

Thiazolidinediones (TZDs) are synthetic peroxisome proliferator-activated receptor γ (PPARγ) agonists that reduce the risk of diabetes by at least 60% in patients with impaired glucose tolerance and/or impaired fasting glucose [20]. In animal studies rosiglitazone administration has been shown to improve glucose homeostasis by improving beta cell function and increasing beta cell mass via reduced beta cell apoptosis [17, 21–23]. The mechanism(s) through which rosiglitazone improves beta cell mass and function are currently unknown but may involve mitochondrial-specific effects. In lymphoma cells, rosiglitazone has been shown to protect against apoptosis by decreasing mitochondria hyperpolarization and increasing ATP production [24]. Furthermore, in adipose tissue, rosiglitazone improves mitochondrial protein expression [25, 26], structure [25], volume and biogenesis [26]. Although these studies suggest that TZDs may target the mitochondria in a variety of tissues, it is currently unknown: (1) whether rosiglitazone can improve the mitochondrial dysfunction observed in beta cells of individuals with type 2 diabetes [5, 9], and (2) by which mechanism rosiglitazone may improve mitochondrial function in beta cells.

Our laboratory has previously established that nicotine exposure during pregnancy and lactation results in loss of beta cell mass at birth, followed by progression from normal to impaired glucose homeostasis in early adult life [27, 28]. Furthermore, fetal and neonatal nicotine exposure was associated with mitochondrial-mediated beta cell apoptosis in neonates [29] and a progressive decline in pancreatic mitochondrial structure and function with increasing age [10]. We have previously demonstrated that early administration of rosiglitazone can prevent the onset of dysglycemia and increase beta cell mass in these animals via reduced beta cell apoptosis [22]. We hypothesize that rosiglitazone improves beta cell mass and function in this animal model by preventing the mitochondrial defects in the pancreas of nicotine-exposed offspring. Furthermore, because IGF1 is thought to preserve beta cell mass and function (reviewed in [19]) and IGF1 treatment has been shown to improve mitochondrial dysfunction and reduce apoptosis in rats [30], we predicted that rosiglitazone might act to improve mitochondrial function indirectly via alterations in the pancreatic IGF axis. Rosiglitazone has been previously shown to alter key components of the IGF axis in bone and liver [31], but its effects on the IGF system in the pancreas have not been examined. Therefore, the primary goal of the current study was to assess the effect of rosiglitazone on mitochondrial structure and function in the pancreas. Second, we investigated whether rosiglitazone may affect mitochondria in the pancreas indirectly via effects on the IGF axis.

Results

Mitochondrial structure and function

The mitochondria in the beta cells of NV (nicotine vehicle) offspring were swollen and consequently, significantly larger than the mitochondria from control offspring (SV; saline vehicle) ($P < 0.05$; Fig. 1a). Postnatal administration of rosiglitazone prevented the nicotine-induced enlargement of mitochondria such that the average mitochondrion area in NR (nicotine rosiglitazone) animals was not significantly different from controls at 26 weeks of age ($P > 0.05$; Fig. 1a). Fetal and neonatal exposure to nicotine resulted in fewer beta cell mitochondria with a healthy, intact inner mitochondrial membrane (i.e., stages 1 and 2) and approximately an 8-fold increase in the proportion of mitochondria that exhibited distention and loss of structural integrity (i.e., stages 3–5) relative to the control (SV) offspring. Rosiglitazone administration to the nicotine-exposed offspring prevented the ultrastructural changes in mitochondrial morphology (Fig. 1b).

Relative to controls (SV), nicotine-exposed offspring had a significant reduction in pancreatic complex IV mitochondrial respiratory chain enzyme activity at 26 weeks of age ($P < 0.05$; Fig. 2). Postnatal rosiglitazone administration from 3 to 26 weeks of age prevented the nicotine-induced inhibition of complex IV activity ($P < 0.05$; Fig. 2). Citrate synthase activity, an indicator of mitochondrial mass, did not differ between the three treatment groups ($P > 0.05$; Fig. 2).

Fetal and neonatal exposure to nicotine resulted in higher levels of mitochondrial DNA (mtDNA) deletions relative to saline-exposed offspring, an effect that was prevented by postnatal treatment with rosiglitazone ($P < 0.05$; Fig. 3).

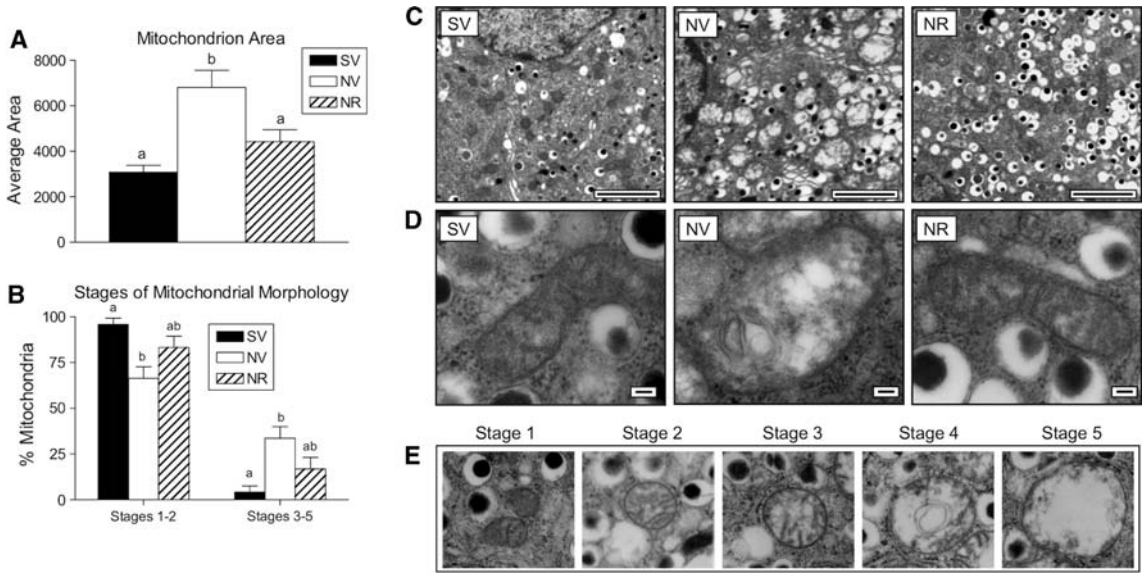

Fig. 1 Electron microscopy of 26 week beta cells (SV: $n = 4$, NV: $n = 5$, NR: $n = 5$). **a** Average individual mitochondrion area within beta cells. **b** Proportion of mitochondria in each of five defined stages of structural degradation (refer to panel **e** for a representative image of mitochondria in each morphological stage, as previously published [10]). Representative EM images from saline vehicle (SV), nicotine vehicle (NV), and nicotine rosiglitazone (NR) treatment groups illustrating mitochondria morphology within beta cells are also provided at **c** 12000× (scale bar = 2 μm) and **d** 120,000× (scale bar = 100 nm) magnification. In panel **d**, a representative "stage 1 mitochondria" is shown for SV and NR animals, compared to a "stage 4 mitochondria" for NV. All data are expressed as the mean ± SEM. Values with different superscripts are significantly different ($P < 0.05$)

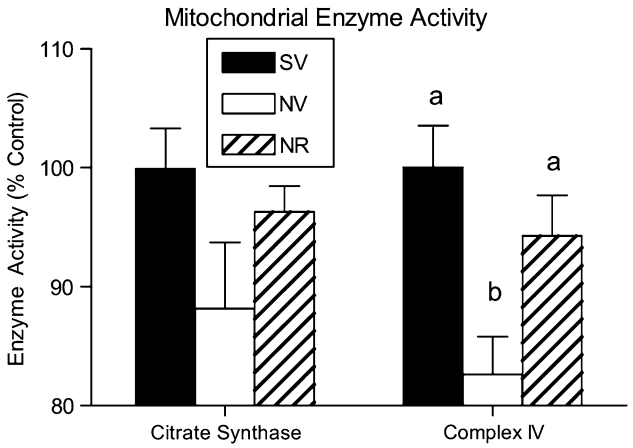

Fig. 2 Mitochondrial enzyme activity (nmol/min/g tissue) in the pancreas at 26 weeks of age, relative to the average saline control value ($n = 5$ per group). Complex IV activity, an indicator of mitochondrial function, and citrate synthase activity, an indicator of mitochondrial mass, were both measured. All data are expressed as the mean ± SEM. Values with different superscripts are significantly different ($P < 0.05$)

Rosiglitazone treatment completely prevented the nicotine-induced inhibition of complex IV activity in beta cell culture (Fig. 4). There was no statistically significant effect of nicotine and/or rosiglitazone treatment on citrate synthase activity in vitro (Fig. 4). Rosiglitazone treatment of healthy (i.e., non-nicotine treated) beta-TC6 cells for 6 or 24 h had no effect on either complex IV or citrate synthase activity at any dose tested (data only shown for 1 μM at 24 h; Fig. 4).

Insulin-like growth factor axis

IGF1 protein expression within the pancreatic islet cells was significantly lower in nicotine-exposed offspring relative to saline controls. This nicotine-induced decline in IGF1 expression was prevented by postnatal rosiglitazone administration (Fig. 5). There was no effect of treatment on IGF2 expression within the islets (Fig. 5).

Relative to saline-exposed controls, fetal and neonatal nicotine exposure caused a significant reduction in pancreatic expression of both the IR and IGF1R, but no change in IGF2R (Fig. 6). Rosiglitazone treatment did not prevent the nicotine-induced dysregulation of either IR or IGF1R expression, but did cause a significant reduction in IGF2R relative to both nicotine- and saline-exposed offspring ($P < 0.05$; Fig. 6).

Discussion

In rats that are prone to developing type 2 diabetes [27, 28], and have known postnatal mitochondrial defects [10], early administration of rosiglitazone increased pancreatic complex IV enzyme activity, reduced the incidence of pancreatic mtDNA deletions and prevented the nicotine-induced

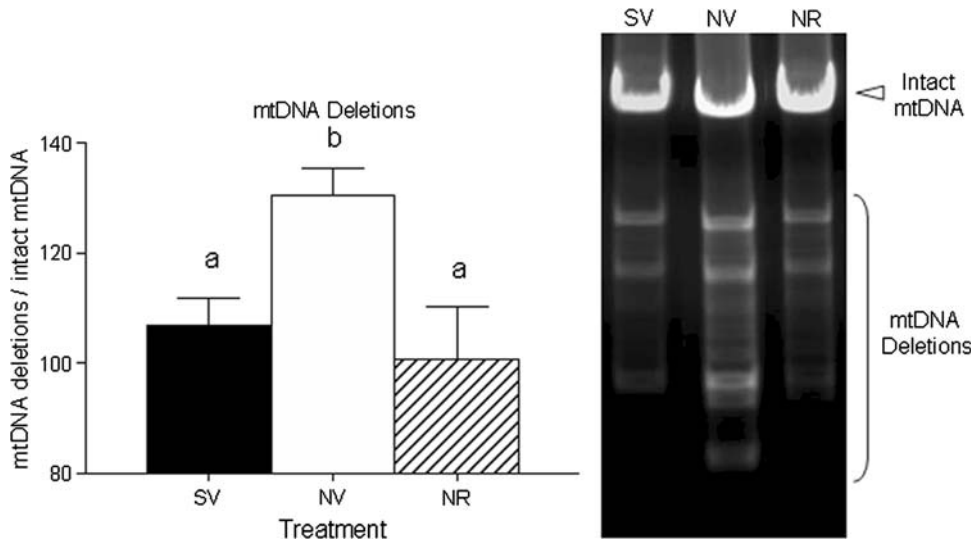

Fig. 3 Mitochondrial DNA deletions in the pancreas at 26 weeks of age ($n = 5$ per group). The upper band represents intact mitochondrial DNA; all bands at a lower molecular weight represent mtDNA with deletions. MtDNA deletions were quantified relative to the intact mtDNA to account for differential loading. All data are expressed as the mean ± SEM. Values with different superscripts are significantly different ($P < 0.05$)

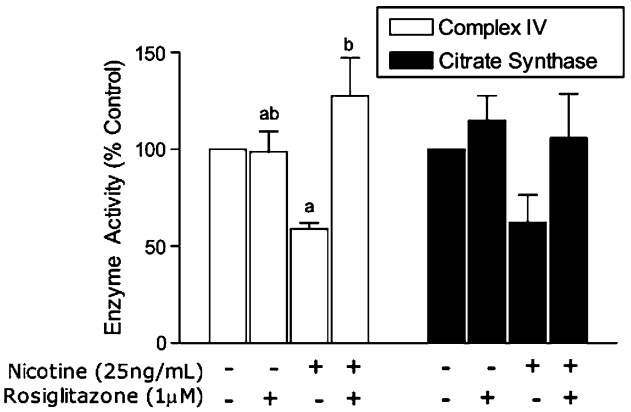

Fig. 4 Complex IV and citrate synthase activity in beta-TC6 cells following in vitro treatment of with vehicle ($n = 6$), 1 μM rosiglitazone alone ($n = 4$), 25 ng/ml nicotine alone ($n = 3$), or both nicotine and rosiglitzone ($n = 4$) for 24 h. All data are expressed as the mean enzyme activity (nmol/min/mg protein) as a percentage of control ± SEM

loss of mitochondrial structural integrity within beta cells. This is the first report to demonstrate that rosiglitazone treatment improves mitochondrial structure and function in the pancreas of diabetes-prone animals.

Mitochondrial structural integrity is an important indicator of mitochondrial function. First, mitochondrial swelling is a key initiating event in the mitochondrial-mediated apoptotic signaling pathway. Second, the enzymes in the electron transport chain (ETC) are located in the inner membrane of the mitochondria and would therefore be affected by impaired membrane structure. We have demonstrated in this study that rosiglitazone improves inner membrane structural integrity and reduces mitochondrial swelling in the beta cells of nicotine-exposed offspring. Similarly, treatment of ZDF rats with the TZD troglitazone decreased the proportion of beta cell mitochondria with visible alterations [32], although no functional consequences of these mitochondrial defects were confirmed. In this study, we have demonstrated that rosiglitazone treatment prevents the loss of complex IV activity in the nicotine-exposed offspring, an indication that mitochondrial respiratory enzyme function has been maintained. Citrate synthase activity was not affected by rosiglitazone treatment, suggesting that the improved mitochondrial function is not simply due to the maintenance of mitochondrial mass. Rosiglitazone administration also prevented the increase in pancreatic mtDNA deletions observed in the nicotine-exposed offspring, another indication that rosiglitazone protects the pancreas from mitochondrial damage. The rate of mtDNA deletions is thought to be almost entirely modulated by the extent of oxidative stress in the mitochondria [3]. Indeed, we have previously demonstrated that nicotine-exposed offspring have elevated levels of reactive oxygen species (ROS) in isolated islets, associated with increased oxidative protein damage compared to saline controls [10, 33]. Therefore, the absence of a nicotine-induced increase in mtDNA deletions with rosiglitazone treatment is suggestive of a reduction in ROS production in the pancreas. Although we have not evaluated the consequences of these mtDNA deletions with respect to the expression of mitochondrial-encoded proteins, it is plausible that these deletions may ultimately affect the transcription of genes that are central to mitochondrial function, and consequently, may impact energy production and cell function.

We hypothesize that the recovery of glucose homeostasis in this animal model [22] is mediated primarily by the ability of rosiglitazone to improve pancreatic mitochondrial respiratory enzyme activity, which would in turn protect both beta cell mass and function. Furthermore, we proposed two different mechanisms through which

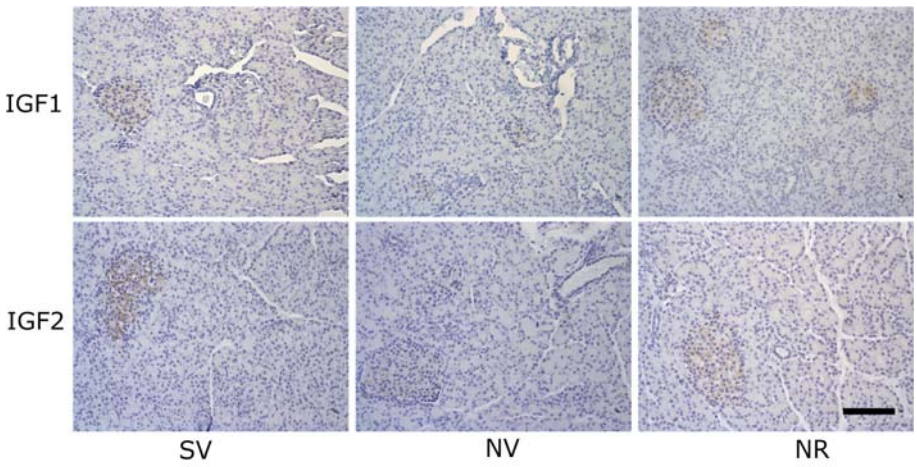

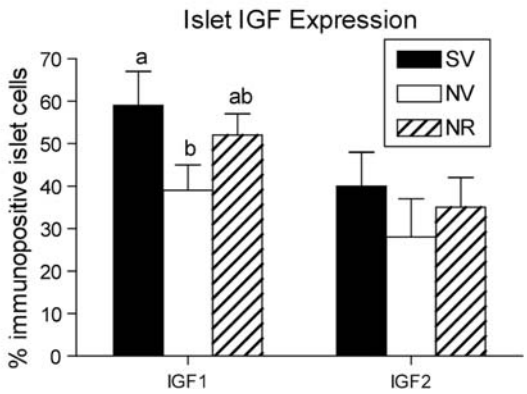

Fig. 5 Immunohistochemical quantification of IGF1 and IGF2 protein expression in pancreatic islets at 26 weeks ($n = 6$ per group). Representative images of immunopositive pancreatic islets are shown from saline vehicle (SV), nicotine vehicle (NV) and nicotine rosiglitazone (NR); scale bar = 100 μm. Data are expressed as the average percentage of immunopositive islet cells ± SEM. Values with different superscripts are significantly different ($P < 0.05$)

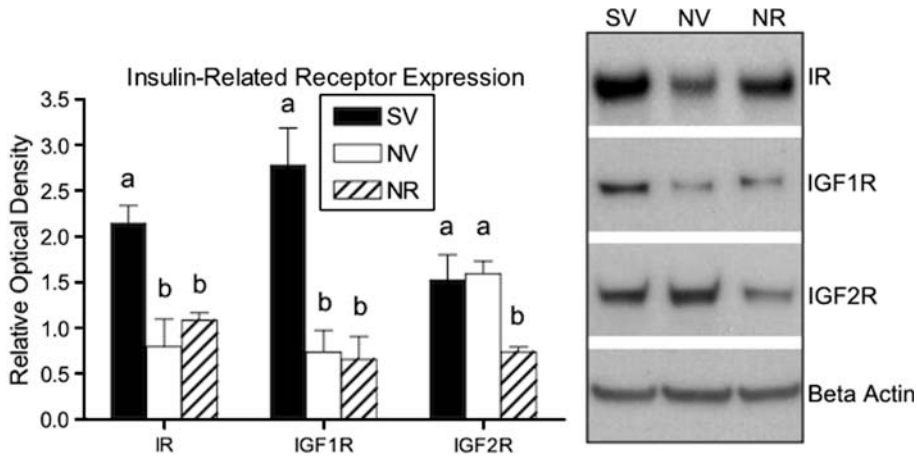

Fig. 6 Representative western blots for insulin-related receptor protein expression in the pancreas at 26 weeks ($n = 4$ per group). Insulin receptor (IR), insulin-like growth factor-1 receptor (IGFR1) and IGFR2 were all quantified in whole pancreas homogenates relative to beta actin as a loading control. Data are expressed as the mean relative optical density ± SEM. Values with different superscripts are significantly different ($P < 0.05$)

rosiglitazone may target pancreatic mitochondria, including: (a) direct action on the pancreatic beta cells, and (b) indirectly increasing IGF signaling.

Rosiglitazone has previously been shown to increase glucose-stimulated insulin release and intracellular ATP content in a rat beta cell line [34]. Therefore, we predicted that rosiglitazone might improve mitochondrial function by acting directly on the beta cell. Interestingly, rosiglitazone treatment (100 nM to 100 μM) of healthy (non-nicotine exposed) beta-TC-6 cells in vitro did not affect either complex IV or citrate synthase activity in this study. However, when mitochondrial function was impaired in beta cells by nicotine exposure, rosiglitazone treatment completely prevented the loss of enzyme activity. These data suggest that the observed improvement of pancreatic mitochondrial structure and function in nicotine-exposed animals treated with rosiglitazone (NR) may be due, in part, to a direct effect of rosiglitazone action on the beta cells.

Recent evidence suggests that the IGF system, composed of the ligands IGF1 and IGF2, as well as the

receptors IR, IGF1R and IGF2R, may be required for protection of mitochondrial function and thus regulation of beta cell survival and function. For instance, knockdown of the IR gene in cardiomyocytes resulted in impaired mitochondrial function and morphology in the heart compared to wild-type mice [35]. Furthermore, treatment of aged rats with recombinant IGF1 improved mitochondrial dysfunction, resulting in reduced mitochondrial free radical production, oxidative damage and caspase-3 activation [30]. Similarly, in humans infused with growth hormone, higher levels of free circulating IGF1 were associated with increased mitochondrial ATP production and improved skeletal muscle oxidative capacity [36]. IGF signaling has also been shown to be essential for regulation of beta cell mass and function (reviewed in [19]). Although our laboratory has recently demonstrated that fetal and neonatal exposure to nicotine can permanently alter expression of key constituents of the intra-ovarian IGF axis [37], the ability of nicotine to impact the pancreatic IGF axis has not been previously examined. Data from this study demonstrate that fetal and neonatal nicotine exposure results in loss of IR and IGF1R protein expression in the adult pancreas, as well as a reduction in islet IGF1 expression. Therefore, the mitochondrial defects in nicotine-exposed offspring are associated with loss of insulin-like growth factor signaling, both of which likely contribute to the loss of beta cell mass and function in this animal model. These results are consistent with the Goto-Kakizaki rat model of type 2 diabetes, which also displays defects in both beta cell mitochondrial structure and function [38], as well as the pancreatic IGF axis [39].

Long-term rosiglitazone treatment slightly attenuated the nicotine-induced reduction in IGF1 protein expression in pancreatic islets, but did not affect either IR or IGF1R expression. Since the actions of IGF1 are mediated primarily by the IGF1R, but can also involve binding to the homologous IR [40], these data suggest that IGF1 signaling in nicotine-exposed offspring was not substantially improved by the rosiglitazone intervention. Rosiglitazone treatment did not affect islet-specific IGF2 protein expression, but did significantly reduce IGF2R expression in the whole pancreas. Since binding of IGF2 to its receptor (IGF2R) leads to degradation of the growth factor [40], these data may indicate increased bioavailability of IGF2 following rosiglitazone exposure. However, protection of beta cell mass and function by IGF2 still relies on cross-reactivity with the IGF1R and IR, which remained significantly reduced in the nicotine-exposed offspring even after rosiglitazone treatment. Taken together, these data indicate that although rosiglitazone may slightly improve IGF signaling in the beta cells of nicotine-exposed offspring due to increased IGF1 expression and IGF2 bioavailability, these alterations are not likely the primary mechanism through which rosiglitazone improves mitochondrial structure and function in diabetes-prone rats.

TZDs have previously been shown to improve glucose homeostasis by maintaining beta cell mass [21, 22]. The loss of beta cell mass and function following fetal and neonatal nicotine exposure has previously been attributed to mitochondrial dysfunction in our animal model [10, 29]. In the current study, we demonstrated for the first time that long-term rosiglitazone exposure improves mitochondrial structure and function in the pancreas of diabetes-prone rats. These alterations may be attributable, in part, to the direct action of rosiglitazone on the beta cell mitochondria, but do not likely involve increased pancreatic insulin-like growth factor signaling. The detailed mechanism(s) by which rosiglitazone can improve pancreatic mitochondrial function remain to be elucidated in this animal model.

Materials and methods

Maintenance and treatment of animals

All animal experiments were approved by the Animal Research Ethics Board at McMaster University, in accordance with the guidelines of the Canadian Council for Animal Care. Nulliparous 200–250 g female Wistar rats (Harlan, Indianapolis, IN, USA) were maintained under controlled lighting (12:12 L:D) and temperature (22°C) with ad libitum access to food and water. Two weeks prior to mating the dams were randomly assigned to receive either saline (vehicle) or nicotine ($n = 20$ per group). Dams were injected with 1 mg kg^{-1} day^{-1} nicotine bitartrate (Sigma–Aldrich, St. Louis, MO, USA) or saline subcutaneously for 14 days prior to mating, and during pregnancy until weaning. Pups were weighed after birth (postnatal day 1; PND1) and litter size was culled to eight at birth. To eliminate any confounding effects of the female reproductive cycle, only male offspring were used in this study. After weaning at postnatal day 21 (PND21), male offspring ($n = 15$ per group) whose mothers had been exposed to nicotine were randomly assigned to receive either vehicle (NV) or rosiglitazone (NR; 3 mg kg^{-1} day^{-1} orally, provided by GlaxoSmithKline, Canada), and male offspring whose mothers were exposed to saline were given vehicle daily (SV). The study was terminated and animals euthanized by CO_2 asphyxiation at 26 weeks of age. Pancreas tissue and serum were collected at necropsy for subsequent analysis.

Electron microscopy

Pancreas tissue was collected from offspring at 26 weeks (SV: $n = 4$, NV: $n = 5$, NR: $n = 5$) and processed for

electron microscopy (EM) as previously described [29]. All chemicals used for electron microscopy were purchased from Canemco Inc., Montreal, QC, Canada unless otherwise stated. Thick sections (approximately 1 μm) were cut on an Ultracut E ultramicrotome (Leica Microsystems, Wetzlar, Germany), stained with toluidine blue and examined under a light microscope to ensure the presence of islets. Thin sections (approximately 70 nm) were then cut from areas of the tissue containing islets, mounted on a Cu/Pd grid (200 mesh), and stained with saturated uranyl acetate and lead citrate. Grids were examined with a JEOL 1200EX transmission electron microscope (JEOL Ltd., Tokyo, Japan) and representative photographs were taken at 12,000× and 120,000× magnification. A minimum of 10 photographs (containing at least 300 mitochondria in the combined fields per animal) were analyzed by a single investigator blinded to the treatment groups using Image Pro Plus Version 5.1 software (Media Cybernetics, Inc., Silver Spring, MD, USA).

Beta cells were identified within the pancreas sections by the presence of insulin granules. Individual mitochondrial morphology was assessed by quantifying: (a) the average mitochondrion area and (b) the proportion of mitochondria in each of five defined stages of progressive deterioration, as previously described [10]. Briefly, stage 1 mitochondria were classified as structurally healthy, with dense, intact cristae. Stage 2 mitochondria had visible swelling, but maintained distinctive intact cristae structure. Stage 3 mitochondria had more severe swelling and minimal evidence of intact cristae. Stage 4 mitochondria displayed severe swelling, minimal cristae structure, and formation of vacuoles. Stage 5 mitochondria were extremely large and swollen, with essentially complete loss of defined structure within the mitochondrial membrane. An example of mitochondria at each defined morphological stage is provided in Fig. 1e.

Mitochondrial enzyme activity

At 26 weeks of age, animals were euthanized by CO_2 asphyxiation, and pancreas tissue was removed, frozen on dry ice and stored at −80°C until analysis. Tissue samples ($n = 5$ per group) were homogenized in homogenization buffer (5 mM HEPES pH 7.4, 100 mM KCl, 70 mM sucrose, 220 mM mannitol, 1 mM EGTA) using Tenbroeck tissue grinders. Homogenates were spun for 10 min at 600×*g*, the supernatant removed, flash frozen in liquid nitrogen and stored at −80°C until use. Citrate synthase activity (an indicator of total mitochondrial mass [41]) was measured using the thiol reagent 5,5′-dithio-bis-(2-nitrobenzoic acid) (DTNB, Sigma Chemical Co., St. Louis MO). Complex IV (cytochrome *c* oxidase) activity was assessed by measuring the rate of cytochrome *c* (from equine heart; Sigma Chemical Co., St. Louis MO) oxidation. Both activity assays were performed using UV-spectrophotometry (Varian Inc., CA) as previously described [10, 42]. Data are expressed as the mean enzyme activity relative to the wet weight of tissue as a percentage of the average saline control value.

Mitochondrial DNA deletions

The presence of random deletions in the mitochondrial DNA (mtDNA) was assessed by the extra-long PCR method, which has been previously described [43]. Briefly, pancreas tissue was removed ($n = 5$ per group), frozen on dry ice and stored at −80°C until analysis. Tissue homogenization and DNA extraction were performed according to manufacturer instructions with the Qiagen QIAamp DNA Mini Kit (Qiagen, CA). mtDNA was amplified using the Expand 20 kb Plus PCR kit (Roche, Mannheim, Germany) and the following primers: FWD 5′-cat agc cgt caa ggc atg aag gtc ag-3′, REV 5′-ggt tgt tga ttt cac gga gga tgg tag-3′ [44]. Reaction mixtures (50 μl final volume) contained 250 ng total cellular DNA, 2 mM dNTPs (Invitrogen, CA), 400 nM of each primer, 5 units of 20 kb plus enzyme mixture (Taq and Tgo DNA polymerases), 1× enzyme buffer and 2.75 mM $MgCl_2$. Amplification was performed in an iCycler Thermal Cycler as follows: (1) 92°C for 2 min; (2) 30× (92°C for 10 s, 62°C for 30 s, 68°C for 20 min); (3) 68°C for 20 min. PCR products were separated on a 0.7% agarose gel and visualized with ethidium bromide. Intact mtDNA appears at 16.5 kb and bands with a lower molecular weight represent mtDNA containing deletions. The optical density of the mtDNA deletion products were quantified relative to the amount of intact mtDNA using Labworks software (UVP Inc., Upland CA). The amount of mtDNA deletions was expressed as the relative optical density (ROD) ± SEM.

Cell culture

The ability of rosiglitazone to directly affect mitochondrial function in pancreatic beta cells was tested in beta-TC-6 cells (a mouse beta cell line; ATCC, Manasas VA). Cells were cultured at 37°C, 5% CO_2 and 95% humidity in Dulbecco's Modified Eagle Medium (DMEM) supplemented with 15% heat inactivated fetal bovine serum (HyClone, Logan, UT). To determine if rosiglitazone has a direct effect on healthy beta cells, dose response curves were generated by treating the cells with increasing log concentrations (100 nM to 100 μM) of rosiglitazone for 6 ($n = 3$ per dose) or 24 h ($n = 4$ per dose). Next, to determine if rosiglitazone has a direct effect on beta cells with nicotine-induced mitochondrial dysfunction, cells were treated with: (a) 1 μM rosiglitazone, (b) 25 ng/ml nicotine, (c) 1 μM rosiglitazone plus 25 ng/ml nicotine, or

(d) vehicle for 24 h. This dose of nicotine is within the range of serum nicotine concentrations reported for active smokers and those smokers using nicotine replacement therapy [45, 46]. Treatments were done in triplicate in a minimum of three independent experiments. Following the 24 h incubation period, cells were washed in Dulbeccos Modified PBS, removed from the plate using cell scrapers (BD Bioscience, Mississauga ON), pelleted by centrifugation and resuspended in homogenization buffer (10 mM Tris–Cl pH 7.4, 250 mM Sucrose and 1 mM EGTA). The cell suspension was sonicated (Microsonix 200) at a low power setting (7 Hz) for 3 10 s bursts. The cell lysates were clarified by centrifugation at $600\times g$ for 5 min at 4°C. The $600\times g$ supernatant was stored at −80°C for further analysis. Cytochrome *c* oxidase and citrate synthase activities were determined as previously described for the pancreas homogenates.

Immunohistochemistry

Islet-specific protein expression of IGF1 and IGF2 in pancreas tissue was determined using immunohistochemistry. Pancreas tissue was removed at necropsy fixed by immersion in 10% (v/v) neutral buffered formalin (EM Science, Gibbstown, NJ) at 4°C overnight, washed in water and embedded in paraffin. Immunohistochemical detection of IGF1 and IGF2 was performed on 5 μm sections ($n = 6$ per group). Briefly, tissues were deparaffinized and rehydrated and antigen retrieval was performed by immersion in 10 mM Citrate buffer (90°C) for 12 min. After inhibition of endogenous peroxidase activity with 2% (vol/vol) hydrogen peroxide, tissues were blocked in 5% (wt/vol) bovine serum albumin in PBS for 10 min. Tissues were then incubated overnight at 4°C in a humidified chamber with anti-IGF1 antibody (1:500 R&D Systems, Minneapolis, MN, USA), anti-IGF2 antibody (1:600, R&D Systems, Minneapolis, MN, USA), anti-IGF1R (1:800 dilution; R&D Systems, Minneapolis, MN, USA), and anti-IGF2R (1:500 dilution; R&D Systems). Anti-sera was diluted in 0.01 M PBS (pH 7.5) containing 2% (wt/vol) BSA and 0.01% (wt/vol) sodium azide (100 μl/slide). All subsequent incubations were at room temperature. Biotinylated anti-rabbit, anti-mouse, or anti-goat IgGs (all 1:100 dilution; Sigma–Aldrich, St. Louis, MO, USA) were diluted in the same buffer and incubated 1 h. The slides were then washed in PBS and incubated with avidin and biotinylated horseradish peroxidase (1:30 dilution) (Extravidin, Sigma Chemical Co, St. Louis, MO, USA). Peptide immunoreactivity was localized by incubation in fresh diaminobenzidine tetrahydrochloride (DAB tablets, 10 mg, Sigma–Aldrich, St. Louis, MO, USA) with 0.03% (vol/vol) hydrogen peroxide for 2 min. Tissue sections were counterstained with Carazzi's Hematoxylin for 1 min. Tissues were dehydrated and placed under a coverslip with Permount (Fisher Scientific, Pittsburgh, PA, USA). Sections were imaged using a brightfield microscope and immunostaining was quantified using image analysis software (ImageScope, Aperio, CA, USA). Staining was quantified as the percentage of immunopositive tissue in four fields of view per section, with a minimum of 6 animals per group.

Western blotting

Protein expression of the key receptors in the IGF axis, including the insulin receptor (IR), insulin-like growth factor receptor 1 and 2 (IGF1R and IGF2R) were measured in whole pancreas homogenates at 26 weeks of age ($n = 4$ per group). Tissue homogenates were prepared as described above. Thirty micrograms of total protein was separated on an 8% polyacrylamide gel and electrotransferred to PVDF blotting membrane (BioRad Laboratories, Hercules, CA). Membranes were blocked overnight with 5% (wt/vol) skim milk in TBST at 4°C and then incubated for 1 h at room temperature in the following primary antibodies: (a) mouse monoclonal IR beta (1:600, 95 kDa, Millipore Corporation, Billerica MA); (b) mouse monoclonal IGF1R (1:250, 130 kDa, Millipore Corporation, Billerica MA); (c) mouse monoclonal IGF2R (1:1,500, 273 kDa, BD Transduction Laboratories, Mississauga, ON, Canada); (d) rabbit polyclonal beta actin (1:8,000, 43 kDa, AbCam, Cambridge, MA). Membranes were cut horizontally at the 55 kDa protein marker; the upper portion was probed for IR, IGF1R or IGF2R, and the lower portion of each blot for beta actin as a loading control. After washing, blots were then incubated in peroxidase-conjugated secondary anti-rabbit antibody (1:2,000; SantaCruz Biotechnology, Santa Cruz, CA) or anti-mouse antibody (1:2,000; Amersham Biosciences, Piscataway, NJ). Reactive protein was detected with ECL Plus chemiluminescence (GE Healthcare Ltd, Buckinghamshire, UK) and Amersham Hyperfilm™ ECL (GE Healthcare Ltd, Buckinghamshire, UK). Densitometric analysis of immunoblots was performed using ImageJ 1.37v 160 software; all proteins were quantified relative to the beta actin loading control.

Statistical analysis

All statistical analyses were performed using SigmaStat (v.3.1, SPSS, Chicago, IL). Data were checked for normality and equal variance and were tested using one-way analysis of variance (ANOVA; $\alpha = 0.05$). The results are expressed as mean ± SEM.

Acknowledgements We thank the staff of the McMaster University Central Animal Facility, Ms Carolyn Cesta, Ms Sandra Stals, Ms Lisa Kellenberger, Mr Ed Hadzocos, and Mr Igal Raizman for their assistance with the animal work. This work was supported by a research grant from GlaxoSmithKline (AVD 103438) to ACH and HCG and funding for the mitochondrial assessment was kindly provided by Mr. Warren Lammert and Ms Kathy Corkins as a donation to Dr. Tarnopolsky. Dr Raha was supported by the Hamilton Health Sciences New Investigator Fund. Dr Gerstein holds the Population Health Institute Chair in Diabetes Research (sponsored by Aventis). Ms Bruin was funded by an Ontario Women's Health/CIHR Doctoral Award, a CIHR Strategic Training Program in Tobacco Research Fellowship, and an Ashley Studentship for Research in Tobacco Control.

References

1. A.E. Butler, J. Janson, S. Bonner-Weir, R. Ritzel, R.A. Rizza, P.C. Butler, Diabetes **52**, 102–110 (2003)
2. P. Marchetti, P.S. Del, R. Lupi, G.S. Del, Nutr. Metab. Cardiovasc. Dis. **16**(Suppl 1), S3–S6 (2006)
3. D.C. Wallace, Annu. Rev. Genet. **39**, 359–407 (2005)
4. D.R. Green, G. Kroemer, Science **305**, 626–629 (2004)
5. P. Maechler, S. Carobbio, B. Rubi, Int. J. Biochem. Cell. Biol. **38**, 696–709 (2006)
6. P.E. MacDonald, J.W. Joseph, P. Rorsman, Philos. Trans. R. Soc. Lond. B Biol. Sci. **360**, 2211–2225 (2005)
7. B.B. Lowell, G.I. Shulman, Science **307**, 384–387 (2005)
8. J.P. Silva, M. Kohler, C. Graff, A. Oldfors, M.A. Magnuson, P.O. Berggren, N.G. Larsson,). Nat. Genet. **26**, 336–340 (2000)
9. M. Anello, R. Lupi, D. Spampinato, S. Piro, M. Masini, U. Boggi, S. Del Prato, A.M. Rabuazzo, F. Purrello, P. Marchetti, Diabetologia **48**, 282–289 (2005)
10. J.E. Bruin, M.A. Petre, S. Raha, K.M. Morrison, H.C. Gerstein, A.C. Holloway, PLoS.ONE. **3**, e3371 (2008)
11. R.A. Simmons, I. Suponitsky-Kroyter, M.A. Selak, J. Biol. Chem. **280**, 28785–28791 (2005)
12. R.N. Kulkarni, J.C. Bruning, J.N. Winnay, C. Postic, M.A. Magnuson, C.R. Kahn, Cell **96**, 329–339 (1999)
13. R.N. Kulkarni, M. Holzenberger, D.Q. Shih, U. Ozcan, M. Stoffel, M.A. Magnuson, C.R. Kahn, Nat. Genet. **31**, 111–115 (2002)
14. K. Ueki, T. Okada, J. Hu, C.W. Liew, A. Assmann, G.M. Dahlgren, J.L. Peters, J.G. Shackman, M. Zhang, I. Artner, L.S. Satin, R. Stein, M. Holzenberger, R.T. Kennedy, C.R. Kahn, R.N. Kulkarni, Nat. Genet. **38**, 583–588 (2006)
15. D. Muller, P.M. Jones, S.J. Persaud, FEBS Lett. **580**, 6977–6980 (2006)
16. K. Robertson, Y. Lu, J.K. De, B. Li, Q. Su, P.K. Lund, J.L. Liu, Am. J. Physiol. Endocrinol. Metab. **294**, E928–E938 (2008)
17. J.C. Devedjian, M. George, A. Casellas, A. Pujol, J. Visa, M. Pelegrin, L. Gros, F. Bosch, J. Clin. Invest. **105**, 731–740 (2000)
18. G. Sesti, A. Sciacqua, M. Cardellini, M.A. Marini, R. Maio, M. Vatrano, E. Succurro, R. Lauro, M. Federici, F. Perticone, Diabetes Care **28**, 120–125 (2005)
19. S.N. Rajpathak, M.J. Gunter, J. Wylie-Rosett, G.Y. Ho, R.C. Kaplan, R. Muzumdar, T.E. Rohan, H.D. Strickler, Diabetes Metab. Res. Rev. **25**, 3–12 (2009)
20. H.C. Gerstein, S. Yusuf, R. Holman, J. Bosch, J. Pogue, Diabetologia **47**, 1519–1527 (2004)
21. D.T. Finegood, M.D. McArthur, D. Kojwang, M.J. Thomas, B.G. Topp, T. Leonard, R.E. Buckingham, Diabetes **50**, 1021–1029 (2001)
22. A.C. Holloway, J.J. Petrik, J.E. Bruin, H.C. Gerstein, Diabetes Obes. Metab. **10**, 763–771 (2008)
23. S.M. Abaraviciene, I. Lundquist, A. Salehi, Cell Mol. Life. Sci. **65**, 2256–2265 (2008)
24. C. Yang, S.H. Jo, B. Csernus, E. Hyjek, Y. Liu, A. Chadburn, Y.L. Wang, Am. J. Pathol. **170**, 722–732 (2007)
25. L. Wilson-Fritch, A. Burkart, G. Bell, K. Mendelson, J. Leszyk, S. Nicoloro, M. Czech, S. Corvera, Mol. Cell. Biol. **23**, 1085–1094 (2003)
26. J.X. Rong, Y. Qiu, M.K. Hansen, L. Zhu, V. Zhang, M. Xie, Y. Okamoto, M.D. Mattie, H. Higashiyama, S. Asano, J.C. Strum, T.E. Ryan, Diabetes **56**, 1751–1760 (2007)
27. A.C. Holloway, G.E. Lim, J.J. Petrik, W.G. Foster, K.M. Morrison, H.C. Gerstein, Diabetologia **48**, 2661–2666 (2005)
28. J.E. Bruin, L.D. Kellenberger, H.C. Gerstein, K.M. Morrison, A.C. Holloway, J. Endocrinol. **194**, 171–178 (2007)
29. J.E. Bruin, H.C. Gerstein, K.M. Morrison, A.C. Holloway, Toxicol. Sci. **103**, 362–370 (2008)
30. J.E. Puche, M. Garcia-Fernandez, J. Muntane, J. Rioja, S. Gonzalez-Baron, C.I. Castilla, Endocrinology **149**, 2620–2627 (2008)
31. B. Lecka-Czernik, C. Ackert-Bicknell, M.L. Adamo, V. Marmolejos, G.A. Churchill, K.R. Shockley, I.R. Reid, A. Grey, C.J. Rosen, Endocrinology **148**, 903–911 (2007)
32. M. Higa, Y.T. Zhou, M. Ravazzola, D. Baetens, L. Orci, R.H. Unger, Proc. Natl Acad. Sci. USA **96**, 11513–11518 (1999)
33. J.E. Bruin, M.A. Petre, M.A. Lehman, S. Raha, H.C. Gerstein, K.M. Morrison, A.C. Holloway, Free Radic. Biol. Med. **44**, 1919–1925 (2008)
34. H.S. Kim, J.H. Noh, S.H. Hong, Y.C. Hwang, T.Y. Yang, M.S. Lee, K.W. Kim, M.K. Lee, Biochem. Biophys. Res. Commun. **367**, 623–629 (2008)
35. S. Boudina, H. Bugger, S. Sena, B.T. O'Neill, V.G. Zaha, O. Ilkun, J.J. Wright, P.K. Mazumder, E. Palfreyman, T.J. Tidwell, H. Theobald, O. Khalimonchuk, B. Wayment, X. Sheng, K.J. Rodnick, R. Centini, D. Chen, S.E. Litwin, B.E. Weimer, E.D. Abel, Circulation **119**, 1272–1283 (2009)
36. K.R. Short, N. Moller, M.L. Bigelow, J. Coenen-Schimke, K.S. Nair, J. Clin. Endocrinol. Metab. **93**, 597–604 (2008)
37. C.E. Cesta, J.J. Petrik, H. Ambraska, A.C. Holloway, Reprod. Biol. Insights **2**, 1–9 (2009)
38. H. Mizukami, R. Wada, M. Koyama, T. Takeo, S. Suga, M. Wakui, S. Yagihashi, Virchows Arch. **452**, 383–392 (2008)
39. S. Calderari, M.N. Gangnerau, M. Thibault, M.J. Meile, N. Kassis, C. Alvarez, B. Portha, P. Serradas, Diabetologia **50**, 1463–1471 (2007)
40. T.W. van Haeften, T.B. Twickler, Eur. J. Clin. Invest. **34**, 249–255 (2004)
41. P.A. Figueiredo, R.M. Ferreira, H.J. Appell, J.A. Duarte, J. Gerontol. A. Biol. Sci. Med. Sci. **63**, 350–359 (2008)
42. G. Parise, S.M. Phillips, J.J. Kaczor, M.A. Tarnopolsky, Free Radic. Biol. Med. **39**, 289–295 (2005)
43. G. Parise, A.N. Brose, M.A. Tarnopolsky, Exp. Gerontol. **40**, 173–180 (2005)
44. J.W. Crott, S.W. Choi, R.F. Branda, J.B. Mason, Mutat. Res. **570**, 63–70 (2005)
45. G.M. Lawson, R.D. Hurt, L.C. Dale, K.P. Offord, I.T. Croghan, D.R. Schroeder, N.S. Jiang, J. Clin. Pharmacol. **38**, 502–509 (1998)
46. S.K. Gupta, S.S. Hwang, D. Causey, C.N. Rolf, J. Gorsline, J. Clin. Pharmacol. **35**, 985–989 (1995)